Meta-analysis reveals the tempo of evolutionary parallelism of local adaptation between native and introduced ranges of plant species

Romane Normand[a,*], Alexis Heckley[b,c], Kathryn Hodgins[d], Samantha Grover[e], Tim Connallon[d,†], Akane Uesugi[a,†]

[a] Department of Biology, School of Science, RMIT University, Bundoora, VIC 3083, Australia
[b] Department of Biology, McGill University, Montréal, Quebec, Canada
[c] School of Biological Sciences, University of Oklahoma, Norman, OK, USA
[d] School of Biological Sciences, Monash University, Clayton, VIC 3800, Australia
[e] Applied Chemistry and Environmental Science, School of Science, RMIT University, Melbourne, VIC 3000, Australia

[*] Corresponding author (romane.r.normand@gmail.com)
[†] Equal contributions

Classification: Biological Sciences/Evolution

Keywords: clinal divergence | parallel patterns | evolutionary predictability | environmental gradients | plant traits

Abstract

Natural selection can cause evolution to be predictable despite the randomness of processes that generate genetic variation. However, the predictability of evolution can be difficult to evaluate, owing to the complexity of environmental conditions that determine selection in each species, and our inability to rewind and replay the tape of life to directly assess evolution's repeatability. Invasive species are valuable systems for evaluating evolutionary predictability, as populations in native and introduced ranges evolve separately, yet often encounter similar environmental challenges, providing potential for parallel patterns of local adaptation between ranges. However, it remains unclear how pervasive such parallelism is, or how rapidly it evolves following species' introductions. To address these questions, we carried out a meta-analysis of clinal divergence in native and introduced populations of the same plant species and evaluated the tempo of evolutionary parallelism of clines between ranges. We show that clinal divergence in introduced ranges was shallower than clinal divergence in native ranges for size, morpho-physiology, and phenology traits, but similar for reproductive and defense traits. Evolutionary parallelism of clinal divergence increased with the age of the species' introduction, with greater parallelism in relatively old introductions caused by increased alignment of the direction of clinal divergence between the ranges rather than changes in the relative magnitudes of divergence in each range. These results suggest a high predictability of local adaptation in mature species' introductions, with drift, genetic constraints and founder effects likely contributing to evolutionary lags in local adaptation within young introductions.

Significance Statement

Species with broad geographic ranges must cope with diverse environments that generate selection for local adaptation. Invasive species are powerful systems for evaluating the rate and ways that species locally adapt, potentially including parallel patterns of trait divergence (clines) within native and introduced ranges. We conducted a meta-analysis of trait clines in native and introduced populations of the same plant species to quantify the tempo and predictability of parallelism between ranges. Introduced populations rapidly re-evolve clines observed within the native range, with degrees of parallelism predicted by the age of the introduction. Strong parallelism emerges within 200 generations following species introductions, owing to increased alignment of cline directions over time. These findings suggest a surprisingly high predictability of local adaptation.

Introduction

A general understanding of the process of adaptation must address several broad questions about how ecology, evolution and genetics interact in natural populations. How predictable is evolution? Do shared environmental conditions lead to reliably parallel evolutionary outcomes (1, 2), or are there multiple genetic or phenotypic solutions to the same environmental challenges (3)? Do populations typically adapt rapidly over ecological timescales (4, 5), or do they experience sustained evolutionary lags in adaptation to their environments, owing to limited genetic variation or other constraints (6, 7)? To what extent does evolution influence ecological dynamics, including expansion, contraction, and fragmentation of species ranges (8–10)? What are the key environmental variables—abiotic and biotic—that determine natural selection and the direction of evolutionary change (11, 12)? Each of these questions is difficult to answer, especially in natural systems.

Invasive species provide exceptional study systems for addressing questions about adaptation, including its predictability, rate, and genetic basis (13, 14). For example, shared environmental factors between the native and introduced ranges of a species can favour parallel local adaptation between ranges ("parallelism"), resulting in geographically similar patterns of spatial divergence along temperature, aridity, or other spatial gradients in the environment (e.g., (15–17)). In other cases, evolutionary contingency or environmental differences between the ranges can promote evolutionary divergence between native versus introduced populations (e.g., (18, 19)). In addition, the age of an introduction constrains the time available for adaptation. In some cases, rapid evolutionary diversification across the new range may keep pace with the range expansion itself, leading to substantial local adaptation within decades of the introduction (20, 21). In other cases, introduced populations may experience evolutionary lags, with protracted periods of suboptimal local adaptation across their introduced ranges (22, 23). Finally, these phenomena may play out differently among trait types (24), which may show

differences in the strength or direction of selection that they experience, or in their genetic capacities for evolutionary change.

Comparisons of native and introduced populations of the same species offer two major advantages for evaluating the evolutionary rate and predictability of local adaptation. First, such studies have a natural, paired design, akin to case-control experiments, in which the evolution of a common set of traits can be directly compared across the native and introduced ranges (25). Such comparisons are particularly powerful when carried out using individuals reared in common garden environments (24), which allows evolved differences among populations to be isolated from environmental factors. One can then directly contrast the direction and steepness of geographic clines across the introduced range, whose populations are relatively young and potentially maladapted to their local conditions, with the native range, whose populations have had extensive time to evolve and are presumably better adapted to local conditions (26, 27). Second, dates of introduction are often well-documented in historical records, which provides opportunities to quantitatively test whether indices of local adaptation (*e.g.*, clines in introduced ranges and parallelism with native range clines) become stronger as the time since the introduction increases (28, 29). If selection favors similar trait–environment relationships in both ranges, older introductions should exhibit greater parallelism than younger introductions (30).

Studies of local adaptation in native versus introduced populations of the same species have progressed to a point where we now have many high-quality case studies spanning a diverse range of plant taxa (24). These studies, if analysed in a common framework, provide an opportunity to test hypotheses about local adaptation, including its degree of parallelism between native and introduced portions of species' ranges, and the tempo with which it evolves following introductions into new ranges. With this goal in mind, we conducted a systematic search for studies of local adaptation in plants and identified 41 studies, spanning 31 species,

that report cline estimates for a total of 586 traits in both the native and introduced portions of the species' range. Of these studies, 34 were conducted in common garden experiments, allowing estimates of genetic clines across populations sourced from different regions of the species' range. Our dataset expands upon earlier meta-analyses of trait clines in native versus introduced plant populations by incorporating studies published over the last 15 years (Colautti and Lau (24) include studies published up to 2011).

We begin with a brief theoretical overview of quantitative predictions for the evolution of clines in native and introduced populations of a species, including the effects of time since introduction, environmental differences between ranges, and evolutionary constraints, on degrees of evolutionary parallelism. We then carry out a detailed analysis of published cline data to address three questions: (1) How predictable is local adaptation, as implied by evolutionary parallelism of trait clines between native and introduced ranges? (2) How rapid is the evolution of local adaptation, as implied by the interaction between the time since introduction and the degree of parallelism between introduced and native populations? (3) To what extent do different trait categories (e.g., morphological, phenological, and defense traits) vary in their degree of parallelism or in their evolutionary lags in introduced ranges?

Trait clines in native versus introduced ranges: Theoretical predictions

Our interpretation of the meta-analysis data relies upon predictions of cline theory from evolutionary quantitative genetics (*e.g.*, (31)), which we outline here and substantially expand upon in the Supplementary Information (SI Appendix 1). We focus here on simple scenarios in which the phenotypic optimum for each trait changes linearly across geographic gradients and local selection is strong relative to drift and gene flow, resulting in strong local adaptation at migration-selection equilibrium in each range. These simplifying assumptions should be viewed as (at best) rough approximations of clinal divergence in real populations.

Consequences of these simplifying assumptions and their violation are briefly discussed below and more thoroughly explored in the SI Appendix 1.

With strong selection relative to gene flow, the evolution of trait clines depends upon the rate at which trait optima change across environmental gradients within each range and whether populations have had sufficient time to evolve to equilibrium. Let B_N and B_I, respectively, represent the spatial rates of change (slopes) of the optima for a single trait across the native and introduced ranges (trait optima are depicted by the dashed lines in Fig. 1A). Native range populations are assumed to be at equilibrium, at which trait clines closely track spatial changes in the optimum (see Fig. 1A, where the slope of the native range cline, b_N, matches the slope of the optimum: $b_N \approx B_N$). Since introduced populations have had less time to evolve within the introduced range, their trait clines (b_I) are more likely to deviate from equilibrium, particularly so immediately following the introduction. The ratio of trait cline slopes in the introduced relative to the native range, over time, can be approximated as:

$$\frac{b_I}{b_N} = \frac{B_I}{B_N}(1 - (1 - h^2\gamma)^t) \tag{1}$$

where h^2 is the trait's heritability, γ is the strength of stabilizing selection around the optimum within each environment, and t is the number of generations since the introduction event.

Under this simple model, the ratio of introduced to native range cline slopes is nearly zero shortly after introduction because populations are not yet locally adapted to the new range (e.g., $b_I/b_N \approx 0$ after $t = 10$ generations in the example from Fig. 1A). Over time, cline slope ratios converge to $b_I/b_N = B_I/B_N$, providing a measure of the degree of parallelism of local adaptation between the native and introduced ranges. ***Perfect parallelism*** between ranges is expected when $b_I/b_N = 1$ at equilibrium. ***Partial parallelism*** is expected when geographic shifts in the optima occur in the same direction between ranges but differ in magnitude

($b_I/b_N > 0$ and $b_I/b_N \neq 1$ at equilibrium). ***Antiparallelism*** arises when trait optima shift in opposite directions between ranges ($b_I/b_N < 0$ at equilibrium). In this model, a strong empirical pattern of parallelism is thus expected when patterns of local selection are similar between ranges and evolutionary lags in local adaptation are quickly resolved. Deviations from perfect parallelism can arise from several factors, including evolutionary lags in local adaptation (which may be strongly influenced by invasion history, including multiple introductions and bottlenecks), divergent patterns of selection between ranges, and differences between ranges in the effects of genetic or demographic constraints to local adaptation (such constraints are explored in the SI Appendix 1; also see: (24, 31, 32)).

Organisms are comprised of many traits that collectively respond to selection, leading to multivariate clinal divergence. Multivariate parallelism between the native and introduced ranges of a species can be quantified by comparing vectors of trait cline slopes from each range. Let $\boldsymbol{b_I} = (b_{I,1}, b_{I,2}, \dots, b_{I,n})$ and $\boldsymbol{b_N} = (b_{N,1}, b_{N,2}, \dots, b_{N,n})$ represent the introduced and native trait cline slopes for the same set of *n* traits. A measure of parallelism between the ranges is:

$$R_P = \frac{\|\boldsymbol{b_I}\|}{\|\boldsymbol{b_N}\|}\cos(\theta) \tag{2}$$

(see Fig. 1B), where the Euclidean norms of the vectors ($\|\boldsymbol{b_I}\|$ and $\|\boldsymbol{b_N}\|$) represent the magnitudes of clinal divergence in each range, θ is the angle between the vectors, and $\cos(\theta)$ represents the correlation (hereafter the "alignment") of cline slopes between native and introduced ranges (also see (33, 34)). Greater Euclidean norms indicate stronger overall clinal divergence across all traits combined, as steeper slopes for any individual trait increase the total magnitude of divergence. In contrast, larger $\cos(\theta)$ indicates that the directions and relative magnitudes of trait slopes are similar between native and introduced ranges. $R_P = 1$ when there is perfect parallelism of local adaptation between ranges (i.e., $\|\boldsymbol{b_I}\|/\|\boldsymbol{b_N}\| = \cos(\theta) = 1$). Deviations from $R_P = 1$ occur when there is a lag in local adaptation across the introduced

range or selection differs between the ranges, leading to differences in the cline magnitudes between ranges ($\|\boldsymbol{b_N}\| \neq \|\boldsymbol{b_I}\|$) and misaligned orientations of cline vectors ($\cos(\theta) < 1$).

The cline estimates included in our meta-analysis are not time-series data, but contemporary snapshots of a clinal divergence in taxa with different residence times within their introduced ranges. To illustrate how evolutionary lags and differences in selection between ranges might influence measures of parallelism in the meta-analysis data, we simulated ratios of introduced and native trait clines (see Fig. 1C-D) across broad distributions of introduction times among species and $h^2\gamma$ values among traits, assuming partial alignment of local selection between ranges (B_N and B_I values were drawn from identical marginal distributions with a modest correlation of 0.5). The simulations ignore effects of estimation error (a feature of real data), invasion-history, genetic drift, and differences between ranges in the strength of genetic or demographic constraints to local adaptation (see the SI Appendix 1 and Discussion). These omissions should result in faster adaptation and stronger parallelism in the simulations than might occur in nature.

Overall, the theory predicts that clines should be shallow in young relative to old introductions, with parallelism between the ranges initially weak ($b_I/b_N < 1$, on average, for small t) but increasing in strength over time ($b_I/b_N = 1$, on average, with large t). Variation of b_I/b_N among traits may, nevertheless, persist (Fig. 1C-D) if traits show variation in the ratio of invasive to native slopes of the trait optima (i.e., if B_I/B_N varies among traits). In multivariate space, parallelism (R_p) is predicted to be weak with young introductions because the magnitude of clinal divergence in the introduced range and its alignment with divergence in the native range are both initially low (Figure A1 in SI Appendix 1). Both factors are predicted to increase with residence time in the introduced range, leading to an increase in parallelism over time, though persistent misalignment in older introductions could indicate sustained selection differences between ranges and/or constraints to local adaptation.

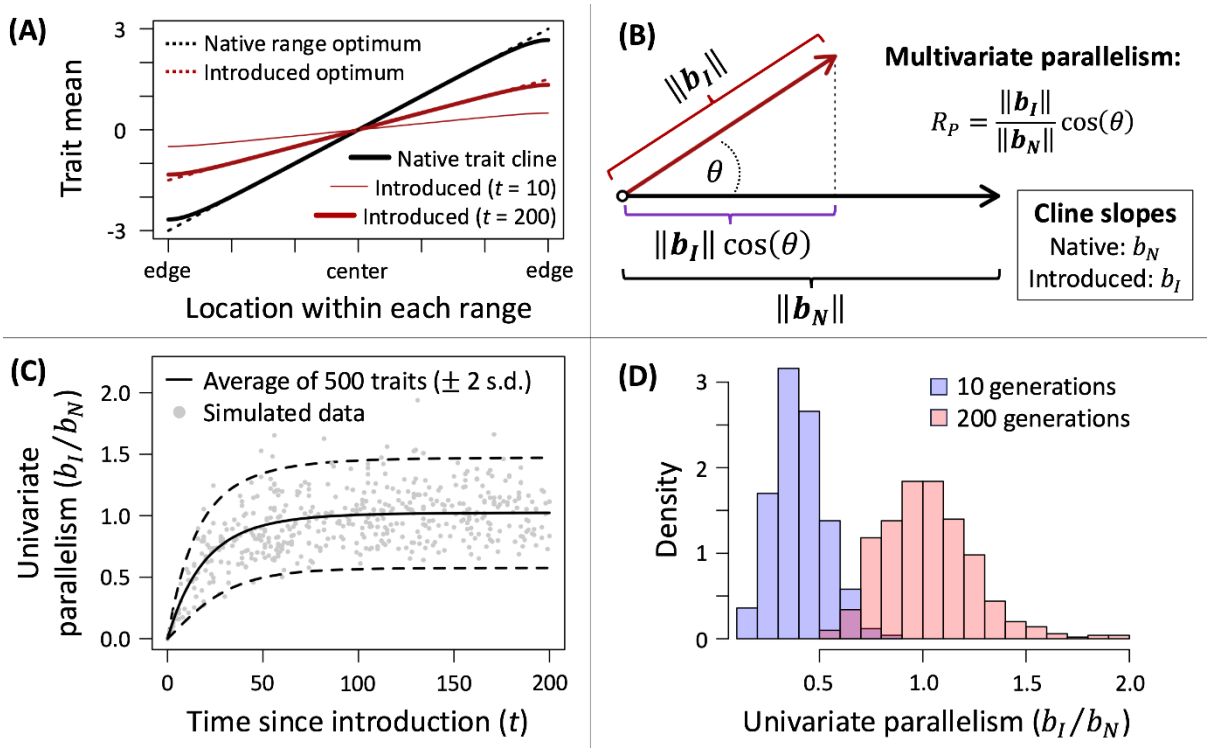

Figure 1. Outline of theoretical predictions for the meta-analysis. **Panel A:** Hypothetical predictions for equilibrium trait clines in the native (black) and introduced populations (red), relative to an introduced cline prior to equilibrium (shortly after introduction). 't' represents the number of generations. Results are based on the uniform population density model presented in the SI Appendix 1(based on (31)), which also presents extensions of the theory that relax some of the simplifying assumptions that apply to the models presented in the main text (*i.e.*, eq. (1) and the surrounding text). **Panel B:** Metrics of multivariate "parallelism" of trait cline slopes. The black arrow represents the magnitude of native cline vector, which is scaled to one. The red arrow shows the magnitude and the direction of the introduced cline vector relative to the native vector. The purple arrow shows the overall degree of parallelism. **Panels C-D:** Simulated data on cline slope ratios for different traits and species with different amounts of time since an introduction into a new range. Simulations of trait cline slopes are based on eq. (1), with $\gamma = 0.1$, h^2 values sampled from beta distribution with a mean of 0.5 and variance of 0.023 (which is compatible with heritability estimates (35), and B_N and B_I values drawn from a bivariate normal distribution with $\mathrm{corr}(B_I, B_N) = 0.5$, and marginal means and variances of $\bar{B}_I = \bar{B}_N = 5$ and $\mathrm{var}(B_I) = \mathrm{var}(B_N) = 1$. **Panel C** shows the univariate parallelism metric (b_I/b_N, as in Panel B) versus time since introduction. **Panel D** shows the distributions of b_I/b_N among traits after 10 and 100 generations of evolution in the introduced range.

Methods

Meta-analysis data

We compiled the meta-analysis data following PRISMA guidelines ((36); see SI Appendix 2, Fig. S1), and included studies reporting trait clines in both the native and introduced ranges of the study species. Eligible articles were identified from searches of Web of Science, Scopus, and PubMed (initial searches were carried out in December 2022 and repeated in May 2025). Keywords were a combination of synonyms related to clines (e.g., "clinal variation"), introduced species (e.g., "introduced"), plant (e.g., "weed"), and the term "adapt*" (see SI Appendix 2, Fig. S1 for details). We included studies using common garden experiments and field surveys published in academic journals with titles and abstracts in English. Studies cited in identified articles were added to our database if they met the inclusion criteria.

When possible, we obtained raw data published online or provided by authors. When raw data were not available, we extracted mean trait values and standard errors from figures using ImageJ (37). Studies with less than four populations were excluded from the analysis. We also excluded studies focusing on 'expanded' ranges, where the native range has recently expanded within the same continent (38). A total of 41 studies met our inclusion criteria. Of those, 29 measured trait variation in a common garden, seven used field surveys, and five used both. One field study (39) examined multiple species within the same localities; we treated each species' dataset as a separate study. Some studies grew plants under multiple common garden treatments (e.g., different water or nutrient regimes) or implemented common garden experiments at different sites. These "experiments" were analysed separately because trait values could not be directly compared across experiments. When multiple introduced ranges were tested against a single native range, we considered each pair of contrasts as a separate "experiment". The final dataset includes paired (native and introduced) cline estimates for 586 traits, from 104 experiments, spanning 31 species and 12 plant families (SI Box S1 and Table

S1). Each trait was classified into one of the following categories (SI Appendix 2, Table S2): morpho-physiology (structural features and functional processes), reproduction (investment in offspring production), size (biomass and growth traits), phenology (timing of developmental stages) and defense (physical and chemical traits that resist herbivory). Species were distinguished by cultivation status (yes/no) using a published dataset (40).

Estimation of the number of generations since introduction

To estimate species' introduction times, we used the specific year of introduction to the study area as provided by authors. When that information was not available, we used the first record of introduction reported by Seebens et al. (41), for countries matching the source populations of each species in our dataset. When records for the source country were unavailable, we used records from the closest country on the same continent. For studies involving populations sampled from multiple countries, we used the average year of the first record across the countries. Years since introduction were calculated as [year of seed collection (or survey in field studies) – year of first record]. When seed collection dates were not available, we used the year when common gardens took place. The number of generations since introduction was calculated as [years since introduction]/[generation time], with species' generation times (in years) obtained from Compagnoni et al. (42). When generation time data were not available, we approximated generation time as $T_z = \alpha + 0.5(\omega - \alpha)$, where α is the species' age at reproductive maturity and ω is the typical lifespan (43), each obtained from TRY database (44). With accurate measures of α and ω, T_z provides a good approximation of generation time (45).

Effect size calculations

All statistical analyses were performed with the R software v.4.4.1 (46) .

Estimation of individual trait cline slopes

For each experiment, we estimated cline slopes using linear models with the population-level trait means as the response variable and the environmental gradient the authors of the original studies focused on as the explanatory variable. These environmental gradients included latitude, principal components of BioClim data, temperature, elevation, aridity, altitude, longitude and soil electrical conductivity. We also analysed the data using a shared environmental predictor across the set of experiments (e.g., by absolute latitude, temperature, and precipitation - the latter two predictors were calculated following Atwater et al. (47)). Within an experiment, traits were standardised (mean = 0; standard deviation = 1) across both native and introduced populations before model fitting. Traits with highly skewed distributions were square root or log transformed prior to standardisation to improve residual normality. For each trait, population means were used to obtain a native slope (b_N), an introduced slope (b_I), and their standard errors. In the following analyses, we focus on ratios of cline slopes (i.e., b_I/b_N and its multivariate analogue), which facilitate comparisons of effect sizes between the wide assortment of traits and study systems in the dataset, regardless of the original units of measurement of the traits or the environmental gradients chosen by the authors.

Multivariate clinal divergence

We carried out multivariate analyses using the 98 experiments with more than one trait. For each experiment, we compiled vectors of introduced and native trait clines ($\boldsymbol{b_I}$ and $\boldsymbol{b_N}$) and calculated their cosine similarity, $\cos(\theta)$, as:

$$\cos(\theta) = \frac{\sum_{i=1}^{n} b_{I,i} b_{N,i}}{\|\boldsymbol{b_I}\| \cdot \|\boldsymbol{b_N}\|}$$

where $b_{I,i}$ and $b_{N,i}$ are the introduced and native slopes of the *i*th of *n* traits in the experiment, and $\|\boldsymbol{b_I}\| = \sqrt{\sum_i^n b_{I,i}^2}$ and $\|\boldsymbol{b_N}\| = \sqrt{\sum_i^n b_{N,i}^2}$ are the total magnitudes of clinal divergence in each range (34, 48). Values of $\cos(\theta)$ are analogous to correlation coefficients, with $\cos(\theta) = 1$ implying a perfect positive correlation, $\cos(\theta) = 0$ implying no correlation, $\cos(\theta) = -1$ implying a perfect negative correlation of cline slopes between ranges. Our measure of multivariate parallelism is $Rp = \|\boldsymbol{b_I}\|\cos(\theta)/\|\boldsymbol{b_N}\|$, as described in eq. (2), with $R_p > 0$ indicating at least partial parallelism between ranges, and $R_p = 1$ with $\cos(\theta) = 1$ indicating perfect parallelism between ranges.

Uncertainty around the point estimates of $\cos(\theta)$ (alignment of clines), $\|\boldsymbol{b_I}\|/\|\boldsymbol{b_N}\|$ (relative magnitudes), and R_p (parallelism), was estimated by bootstrapping the original data by randomly selecting individual samples with replacement. For each bootstrapped sample, we used population means of trait values to calculate the parameters using the methods described above. In cases where only population means and standard errors were available (but not the raw data), we simulated trait means for each population by pseudo-random sampling from a normal distribution with mean corresponding to the point estimate of the mean for the population and standard deviation corresponding to its standard error. Each set of simulated means across populations within a range was used to calculate cline slopes, from which we recalculated the multivariate parameters. We repeated this process 10,000 times to approximate confidence intervals for these parameters.

Univariate clinal divergence

To examine cline parallelism for different trait categories, we carried out univariate analyses using estimates of the b_I/b_N ratio, per trait, using the linear models. Our univariate analyses

focus on traits with statistically significant clines in at least one range (336 of 586 traits in the dataset), as those without a significant cline in either range are irrelevant to tests of parallelism.

Following Friedrich et al. (49), we analysed the natural logarithm of cline slope ratios, which facilitates parametric statistical analyses of meta-analysis effect sizes. Logarithms of negative numbers are undefined, and a substantial proportion of b_I/b_N ratios in the dataset were negative. We dealt with this issue by first analysing ratios of absolute values ($|b_I/b_N|$), which quantify the relative magnitudes of clines but ignore similarities/differences in cline directions, and separately analysing b_I/b_N ratios of traits with clines slopes of the same sign, for which $\ln(b_I/b_N)$ has a defined value. 95% confidence intervals for the mean of $\ln(|b_I/b_N|)$ and $\ln(b_I/b_N)$ were calculated using equations presented by Friedrich et al. (49). Systematic differences between native and introduced cline slopes correspond to cases where 95% confidence intervals of the pooled effect sizes do not overlap with zero.

To test whether the proportion of clines going in the same direction ($b_I/b_N > 0$) changes with the number of generations since introduction, we built a generalised linear model (*glm*) with generations-since-introduction as the fixed effect, a binomial error distribution and a logit link function, and a binary response variable ($0 = [b_I/b_N < 0]$ and $1 = [b_I/b_N > 0]$).

Meta-analysis overview

All meta-analyses were performed using the function *rma.mv* from the package 'metafor' (50). Parameters in the meta-analytical models were estimated using restricted maximum likelihood (51), with Knapp-Hartung adjustments used to calculate the confidence interval of pooled effects (52). We performed multilevel random-effects models to account for the hierarchical structure of non-independence in our dataset (multiple traits in multiple experiments within single studies; multiple studies examine the same species). We used the function *var.comp* from the package 'dmetar' (53) to calculate the total heterogeneity (I^2), and heterogeneity at each

357 level ($I^2_{level\ 2}$ and $I^2_{level\ 3}$). We tested whether residual heterogeneity was due to sampling error
358 only using the QE statistic, with significant QE indicating that residual heterogeneity can be
359 explained by factors not included in the model (50).

360 The meta-analysis of multivariate parameters estimated pooled effect sizes and 95%
361 confidence intervals for $\cos(\theta)$, $\|\boldsymbol{b_I}\|/\|\boldsymbol{b_N}\|$, and R_p, with random effects of study identity
362 nested within a species. We tested for relationships between multivariate parameters and the
363 number of generations since introduction by including generations since introduction,
364 alongside method (common garden experiment vs. field surveys), cultivation status, and
365 number of traits, as moderators. We generated models with all combinations of these
366 explanatory variables as main effects, and with pairwise interactions considered only for
367 generations-since-introduction using the function *glmulti* (package 'glmulti' (54)) and selected
368 the best model based on Akaike information criterion with small sample size correction (AICc).
369 Models within ΔAICc < 2 were considered competitive (55), and we compared the model-
370 averaged importance of each term within the competitive model set to determine the final
371 model structure.

372 For the univariate analysis, random effects of experiment identity, nested within the
373 study identity, accounted for within- and between-study heterogeneity. Species identity was
374 removed from the models because the multivariate analysis revealed little heterogeneity
375 explained by species identity. Following the same method as before, we examined how trait
376 category, method, cultivation status, generations-since-introduction and pairwise interaction
377 with the latter affected the extent of parallelism between native and introduced ranges. The
378 package 'orchaRd' was used for graphical purposes (56).

379

380

Results

Multivariate analysis of clinal divergence

Across experiments, we found partial, but significant (t_{97} = 4.2, P < 0.0001), parallelism between native and introduced clines (the mean pooled effect size of R_p was 0.28, i.e. 28% of what is expected under perfect parallelism, with 95% CI [0.15, 0.41]; Fig. 2A). The alignment of native and introduced range vectors ($\cos(\theta)$) was positive in 65% (64 of 98) of experiments, indicating that native and introduced populations tend to clinally diverge in similar directions ($\chi^2 = 4.1, P = 0.04$). The mean alignment between native and introduced cline vectors was $\cos(\theta) = 0.30$ ([0.15, 0.45], t_{97} = 4.1, P < 0.0001), while the ratio of the cline vector magnitudes ($\|\boldsymbol{b_I}\|/\|\boldsymbol{b_N}\|$) was 0.73 ([0.60, 0.86], t_{97} = 11.3, P < 0.0001), indicating that introduced populations show relatively strong clines (73% of native cline magnitudes) that are weakly aligned with the native clines. Residual heterogeneity (i.e., QE) was significant, primarily due to study identity in all three metrics (SI Appendix 2, Table S3).

Variation in R_p and $\cos(\theta)$ was best explained by the additive effects of generations since introduction and study method (SI Appendix 2, Table S4). R_p increased with the number of generations since introduction (*slope* = 0.0051, t = 3.7, P = 0.0004, Fig. 2B) and was higher in common gardens than field surveys (t = 3.0, P = 0.004). Similarly, $\cos(\theta)$ increased with introduction time (*slope* = 0.0030, t = 2.7, P = 0.008, Fig. 2C) and was higher in common gardens than field surveys (t = 3.3, P = 0.001). In contrast, none of the moderators we examined, including generations since introduction, explained variation in $\|\boldsymbol{b_I}\|/\|\boldsymbol{b_N}\|$ (*slope* = 0.0013, t = 1.1, P = 0.28, Fig. 2D). These results indicate that the increase in parallelism with time since introduction is primarily due to increasing alignment of clines rather than changes in their relative magnitudes.

The above results are based on clines associated with the spatial or environmental gradients chosen by the original study's authors (most chose latitude, though some used

predictors like temperature, precipitation, or aridity). To evaluate the robustness of our results, we repeated the multivariate analyses using re-estimated trait clines predicted by absolute latitude, or gradients of temperature or precipitation. Results for R_p, $\cos(\theta)$, and $\|\boldsymbol{b_I}\|/\|\boldsymbol{b_N}\|$ were similar for each predictor of clinal divergence, though clines across precipitation gradients resulted in overall quantitatively weaker degrees of parallelism relative to other gradients (SI Appendix 2, Table S5). Associations with time since introduction remained significant for latitudinal clines, but not for clines predicted by temperature or precipitation gradients (SI Appendix 2, Table S6).

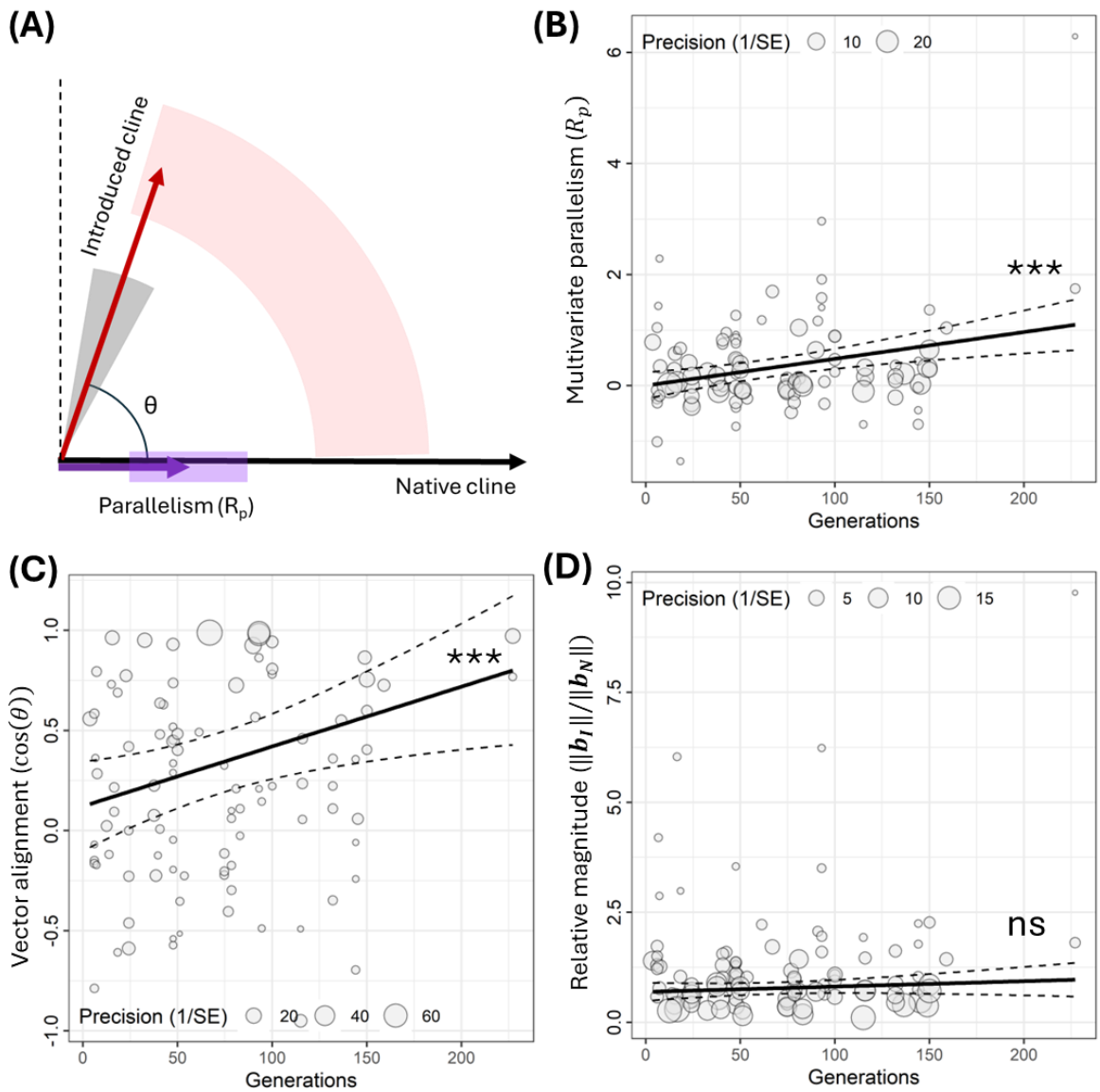

Figure 2. Multivariate clinal divergence between introduced and native ranges. **(A)** Cline vectors of native and introduced ranges are presented as arrows (black and red, respectively), with the angle between the vectors (θ) indicating their mean degree of alignment across studies. The length of the introduced vector represents the mean magnitude of introduced vector relative to that of the native vector ($\|\boldsymbol{b_I}\|/\|\boldsymbol{b_N}\|$), where the native vector magnitude is scaled to one ($\|\boldsymbol{b_N}\| = 1$). Grey shading denotes the 95% CI of θ, and pink shading denotes the 95% CI of $\|\boldsymbol{b_I}\|/\|\boldsymbol{b_N}\|$. The purple arrow indicates the degree of multivariate parallelism between ranges (R_p), with shading denoting its 95% CI. An arrow length greater than 0 and less than 1 indicates partial parallelism. **Panels B-D** show the associations between the number of generations since introduction and **(B)** R_p, **(C)** cos(θ), and **(D)** $\|\boldsymbol{b_I}\|/\|\boldsymbol{b_N}\|$, with meta-analytic data shown as bubble plots. Asterisks indicate a significant association with time (*** $P < 0.0001$).

Univariate analysis of divergence across different trait categories

Among the 336 traits with a significant cline in at least one range (Fig. 3), 197 (59%) were in the same direction ($b_I/b_N > 0$) and 139 (41%) were opposite ($b_I/b_N < 0$). Native clines were, on average, steeper than introduced clines, with the magnitude of introduced clines being 71% of their native counterparts (mean $\ln(|b_I/b_N|)$ = -0.34, 95% CI = [-0.55, -0.13]). Residual heterogeneity (i.e., QE) was significant, primarily due to study identity (SI Appendix 2, Table S3).

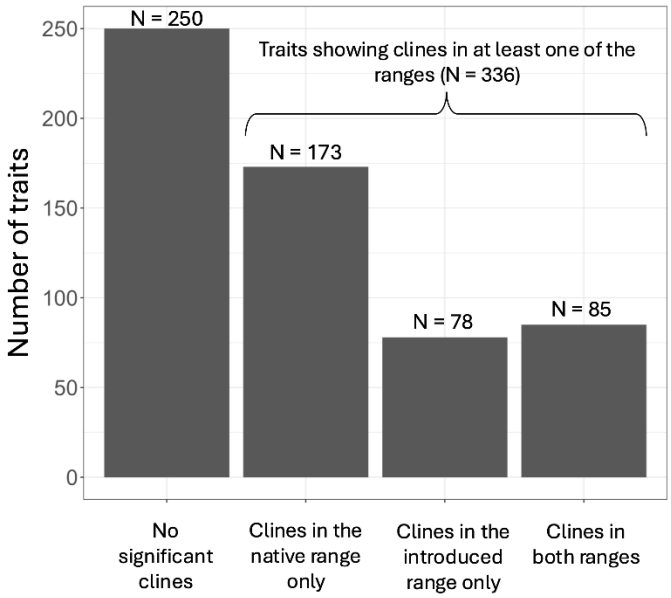

Figure 3. Results of the linear model tests for clinal variation in 586 traits of the meta-analysis. Slope estimates were (left to right): non-significant in both ranges, significant in the native range only, significant in the introduced range only, or significant in both ranges.

Model selection revealed that variability in $\ln(|b_I/b_N|)$ was best explained by 'trait category' alone (SI Appendix 2, Table S4). The magnitude of clinal divergence was similar between ranges for defense and reproductive traits, with introduced clines showing 127% and 86% the magnitude of native clines, respectively ($\ln(|b_I/b_N|) = 0.24$ [-0.15, 0.63] and $\ln(|b_I/b_N|) = -0.15$ [-0.43, 0.12]). In contrast, clinal divergence was systematically shallower for morpho-physiology (51%, $\ln(|b_I/b_N|) = -0.67$ [-1.01, -0.32]), phenology (52%, $\ln(|b_I/b_N|) = -0.65$ [-0.94, -0.35]), and size traits (55%, $\ln(|b_I/b_N|) = -0.60$ [-0.85, -0.34]).

While the relative magnitude of clinal divergence in each range was not associated with the time since introduction (*slope* = 0.0007, t = 0.0019, $P = 0.73$; Fig. 4C), the proportion of clines diverging in the same direction increased with time (*slope* = 0.009, z = 0.002, $P = 0.0002$; see Fig. 4D). This increase holds qualitatively for each trait category analysed separately, though interactions with time were only significant for the size-related traits (SI Appendix 2, Fig. S2), possibly owing to the smaller sample sizes of other categories.

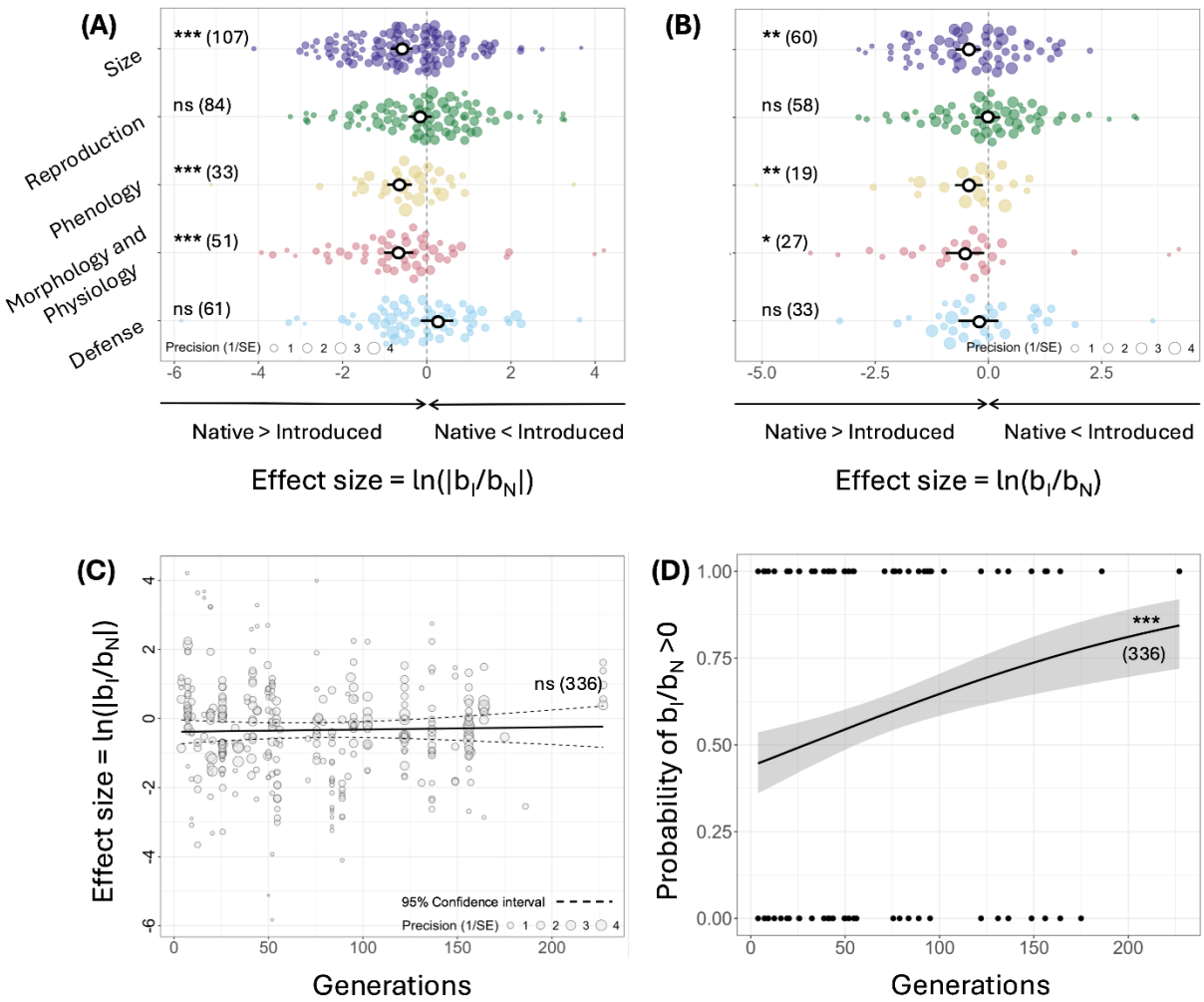

Figure 4. Univariate estimates of parallelism between native and introduced ranges. **Panels A-B** show the absolute ratio of introduced to native slopes in log scale ($\ln(|b_I/b_N|)$), analysed separately for each trait category. **(A)** includes values of all traits, and **(B)** includes only traits whose cline estimates diverge in the same direction ($b_I/b_N > 0$). The mean effect sizes (white circles) are plotted with the 95% confidence intervals (bold line), with the number of traits given in brackets (SI Appendix 2, Table S7). Asterisks indicate significant deviation from $\ln(|b_I/b_N|) = 0$ (perfect parallelism). The individual effect sizes (coloured circles) for five trait categories are plotted with circle size denoting precision (inverse variance). **Panels C-D** show the relationship between the number of generations since introduction and **(C)** cline slope ratios, or **(D)** the probability that clines in each range diverge in the same direction (*i.e.,* $b_I/b_N > 0$, analysed using a generalized linear model). Asterisks indicate a significant association with time. * $P < 0.05$, ** < 0.01, *** < 0.0001.

Similar results apply for the 197 traits with cline estimates diverging in the same direction (traits where $b_I/b_N > 0$; Fig. 4B). In these cases, magnitudes of introduced clines were 76% of the magnitudes of native clines ($\ln(b_I/b_N)$ = -0.28 [-0.50, -0.06], SI Appendix 2, Table

S3). Cline slopes were similar between introduced and native ranges for defense traits (80%, $\ln(b_I/b_N)$ = -0.22 [-0.67, 0.22]) and reproductive traits (99%, $\ln(b_I/b_N)$ = -0.01 [-0.29, 0.27]), while clines were shallower in introduced ranges for morpho-physiology (59%, $\ln(b_I/b_N)$ = -0.52 [-0.94, -0.09]), phenology (65%, $\ln(b_I/b_N)$ = -0.43 [-0.74, -0.12]), and size traits (64%, $\ln(b_I/b_N)$ = -0.45 [-0.73, -0.17]). There was no association between $\ln(b_I/b_N)$ and the number of generations since introduction (SI Appendix 2, Fig. S3).

Discussion

Our meta-analysis reveals three broad patterns of evolutionary parallelism between the trait clines of native versus introduced ranges. First, multivariate parallelism (R_p) across the entire dataset is relatively low, overall—on average, only 28% of the divergence predicted under perfect parallelism. This low average R_p was due to shallower clinal divergence in introduced relative to native ranges ($\|\boldsymbol{b_I}\|/\|\boldsymbol{b_N}\| = 0.73$) along with a modest alignment of cline directions between ranges ($\cos(\theta) = 0.30$). Second, multivariate parallelism between ranges markedly increases with the residence time of introduced populations (generations since introduction), resulting in strong parallelism between ranges involving relatively old introductions (i.e., $R_p \approx 1$ at 200 generations post introduction; Fig. 2C). This increase in parallelism over time is primarily caused by increased alignment of cline directions between ranges rather than changes in relative cline magnitudes. Third, degrees of parallelism between ranges vary among traits, and are stronger for reproductive and defense traits than for phenological, morpho-physiological, and size-related traits; the latter three categories exhibit weaker clines in introduced ranges. Below, we discuss processes that might explain these observations before outlining opportunities for future work.

Why are trait clines shallower in introduced ranges?

Several evolutionary mechanisms could contribute to shallower clines in introduced relative to native ranges (*i.e.*, $\|\boldsymbol{b_I}\|/\|\boldsymbol{b_N}\| < 1$). Under simple theoretical models that assume strong selection and no genetic or demographic constraints (Fig. 1), shallower clines in introduced ranges can emerge from time lags in local adaptation (57), or shallower underlying environmental gradients in introduced range (*i.e.*, $|B_I/B_N| < 1$; recall that B_I and B_N refer to slopes of changes in trait optima). The time-lag hypothesis predicts an increase in $\|\boldsymbol{b_I}\|/\|\boldsymbol{b_N}\|$ with the residence time of introduced populations—a pattern that we did not observe. Alternatively, environmental gradients might be shallower in introduced ranges if species are disproportionately introduced into geographic regions where the environmental gradients are relatively shallow, which would facilitate range expansions in those regions (58). For example, urban environments that many invasive plants occupy (59) may provide more homogeneous landscapes than natural systems (60). Unfortunately, direct comparisons of environmental gradients between native and introduced ranges are lacking, making it difficult at present to formally evaluate this hypothesis.

A more complex picture emerges in the presence of genetic, evolutionary, and demographic factors that constrain local adaptation, potentially leading to shallower clines in introduced ranges. For example, weaker selection and/or lower genetic variation in introduced ranges would enhance the swamping effects of gene flow on clinal divergence, resulting in shallower clines at migration-selection balance. However, heritability estimates for fitness-related traits (61–65) and linear selection gradients (24) generally have similar magnitudes in native and introduced ranges, offering little support for this explanation, though such data are admittedly sparse.

Demographic differences between ranges—including differences in the rate of dispersal or the spatial distribution of population density (see SI Appendix 1)—can also lead to different

degrees of swamping of local adaptation between ranges. Invasive herbaceous plant species tend to have higher dispersal rates than non-invasive ones (66), and increased dispersal ability can evolve within introduced ranges (61, 67), which could lead to higher swamping by gene flow in introduced ranges relative to native ranges. The distribution of population density affects local adaptation by mediating the rate of gene flow from the center of a range to its edges, with 'abundant center' distributions leading to much stronger swamping than under relatively uniform patterns of population density across a range (31). Introduced populations that more closely conform to an abundant-center scenario than do their native counterparts (which might be likely in actively expanding introductions; (68)) will be more susceptible to swamping.

Strong genetic correlations between traits can further constrain rates of local adaptation and greatly extend time lags in local adaptation but nevertheless lead to weak associations between the relative magnitudes of clinal divergence in each range and the time since introduction (Fig. 5). Figure 5A illustrates one such example, where $\|\boldsymbol{b_I}\|/\|\boldsymbol{b_N}\|$ for two strongly correlated traits is relatively flat across the first 200 generations of evolution in the introduced range, though the increase is much more visible over longer time intervals. We return to this point in the following section.

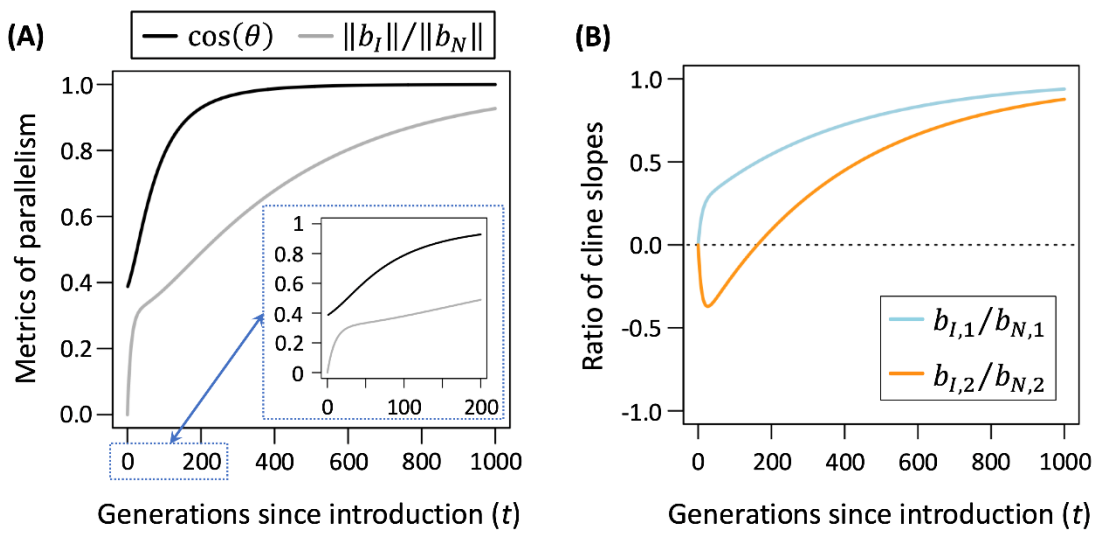

Figure 5. Evolution of clines for a pair of genetically correlated traits. The plots show a scenario in which the optima for the pair of traits shift in opposite directions, with $B_1 = 2$ and $B_1 = -1$, and the traits are otherwise subject to the same strength of stabilizing selection ($\gamma = 0.05$). Heritability for each trait is $h^2 = 1$ and the genetic correlation between the traits is strongly positive ($\rho = 0.95$). Parameters of selection and variation are assumed to be identical between the native and introduced ranges, so that perfect parallelism ($\|\boldsymbol{b_I}\|/\|\boldsymbol{b_N}\|$ and $\cos(\theta) = 1$) is predicted at equilibrium. Panel **(A)** shows the evolution of $\cos(\theta)$ and $\|\boldsymbol{b_I}\|/\|\boldsymbol{b_N}\|$ across 1000 generations since the introduction at generation $t = 0$, with the inset highlighting the predictions for the first 200 generations. Panel **(B)** shows the evolution of clines for each trait—including a counter-cline that arises early for trait 2 but ultimately resolves as introduced populations approach migration-selection equilibrium. Details of the model can be found in SI Appendix 1.

The trend towards shallower slopes in introduced ranges does not, however, apply across the board. Defense and reproductive traits have similar cline magnitudes between ranges, while clines for phenological, morpho-physiological, and size-related traits were shallower (roughly half as steep) in introduced relative to native ranges. These differences among trait categories might stem from differences in evolutionary potential for rapid local adaptation, with traits under exceptionally strong selection or with high heritabilities evolving more rapidly in introduced ranges. Reproductive traits, for example, are thought to be under strong selection because they are closely related to fitness (69, 70). Likewise, the average heritability of plant secondary metabolites (which includes defensive compounds) is estimated to be more than twice as large as the heritability of phenological, morphological, physiological, and size traits, which should facilitate responses to selection ((71); see also (61, 72)).

Why does the alignment of cline directions between ranges increase over time?

Four factors potentially contribute to the weaker alignment of cline directions in younger than older introductions (recall that $\cos(\theta)$ quantifies alignment between ranges). First, traits differ in how responsive they are to natural selection: those with high heritability and under strong

selection will rapidly adapt to local conditions across the new range, while those with low heritability or weak selection should exhibit protracted lags in local adaptation (see the SI Appendix 1). This heterogeneity of lag-times among traits leads to temporary misalignments in the relative magnitudes of clines in each range, which eventually resolve as each trait evolves to migration-selection equilibrium in the new range. However, while this scenario might contribute to the temporal increase in alignment that we observe, it is unlikely to be the only explanation, since this scenario also predicts a concurrent, and much larger, increase in $\|\boldsymbol{b_I}\|/\|\boldsymbol{b_N}\|$, which we do not observe (see Fig. A1, SI Appendix 1), nor can it account for the high proportion of counter-clines in young introductions.

Second, in the early stages of invasion, stochastic processes can play important roles in the initial formation of clines. Founder effects and genetic drift during range expansion can produce clines in random directions (24), many of which will not align with those in the native range. Similarly, spatial sorting of dispersal-related traits during expansion, documented in both plants and animals (see (73) for review), can create gradients that are potentially correlated with environmental variables but primarily reflect colonisation history rather than local adaptation. Furthermore, multiple introductions from genetically divergent source populations, or hybridisation, could generate irregular or even counter-clines, particularly in younger invasions where admixture between lineages is ongoing. If selection pressures are similar between ranges, these stochastic and historical effects on the initial formation of clines are expected to diminish over time, as natural selection reorients clines to align with those maintained in the native range, leading to the observed increase in parallelism among the older introductions.

Third, the directions of selection in each range might change over time, leading to a greater alignment of both selection and trait clines in old relative to young introductions. For example, selection may fundamentally differ between young and old introductions if the former

experiences a release from natural enemies, but the latter does not. Enemy release might relax selection of defense traits within the new range and facilitate evolution of defense trait clines caused by drift or by indirect responses to selection of genetically correlated traits (as predicted by the "evolution of increased competitive ability" (EICA) hypothesis (74)). Moreover, relaxation of herbivory may alter the pattern of selection on secondary metabolites with dual functions in herbivore defense and abiotic stress tolerance (28), with metabolite concentrations in recently introduced species evolving in response to selection for abiotic stress tolerance rather than herbivore defense (28). Clines favoured by selection in young introductions may, thus, differ substantially from those in the native range. However, subsequent accumulation of natural enemies in the introduced range over time (75, 76) may gradually reshape the selective landscapes of older introduced ranges, leading to a stronger alignment of selection and evolutionary parallelism of clines between native and introduced ranges.

Finally, strong genetic correlations between traits can both constrain the rate of local adaptation in introduced ranges and lead to transient counter-clines in traits subject to relatively weak selection (Fig. 5B). Under such conditions, $\|\boldsymbol{b_I}\|/\|\boldsymbol{b_N}\|$ for a set of traits can rapidly increase soon after the introduction and then remain evolutionarily stagnant due to genetic constraints to further local adaptation of each trait, whereas the alignment of the clines from each range steadily increases over the same time interval (see the inset of Fig. 5A). Strong parallelism of clines (e.g., $\|\boldsymbol{b_I}\|/\|\boldsymbol{b_N}\| \approx \cos(\theta) \approx 1$) can ultimately evolve between the native and introduced ranges, yet strong genetic constraints can draw out this process and, depending on the time window of the observation, reveal a pattern in which $\|\boldsymbol{b_I}\|/\|\boldsymbol{b_N}\|$ is relatively constant over time while $\cos(\theta)$ steadily increases, as found in our meta-analysis. Strong genetic correlations and trade-offs between fitness-related traits may indeed be likely. For example, both early flowering and large biomass (and seed production) are favoured at

high latitudes, yet these traits negatively covary, providing the potential for the evolution of transient counter-clines in the more weakly selected trait (see (22, 77)).

Conclusions and future directions

A trait or allele frequency cline is not, in itself, evidence for local adaptation (24). However, repeated evolution of parallel clines between geographically disjunct regions of a species' range is difficult to reconcile with nonadaptive explanations and is instead indicative of repeated local adaptation to shared environmental conditions between the regions (78, 79). We found that geographic clines in plant traits showed strong evolutionary parallelism between native and introduced ranges with relatively long residence times (on the order of 100 or more generations). This result applies to a broad set of plant species and trait types and implies that local adaptation is extensive and predictable across native ranges and mature introduced ranges.

More surprisingly, our analysis suggests that the greater parallelism of older relative to younger introductions is primarily due to an increase in the alignment of cline directions between ranges rather than changes to the relative magnitudes of clines in introduced versus native ranges—a pattern that holds qualitatively across different trait categories. Although several factors may contribute to this pattern, we suspect it is caused by rapid evolution of maladaptive clines for a subset of traits in young introductions—owing to processes like drift, founder effects, and spatial sorting during colonization, or to indirect responses to selection of genetically correlated traits. This is followed, in the longer term, by more gradual evolution of local adaptation that results in increased parallelism between clines in each range. Direct tests for enrichment of maladaptive clines in young relative to old introductions (e.g., through estimates of selection of clinally diverging traits) would, therefore, be a worthwhile focus for future work. Other potentially useful extensions of our study include analyses of nonlinear clines (which are sometimes reported in cline studies, e.g., (15, 80)) and their evolutionary

parallelism between ranges, and analyses of the joint tempo of changes in trait clines and the geographic breadths of introduced species' ranges, both of which may increase over time, with adaptive clines possibly facilitating expansions of range breadth (58).

Finally, we used a snapshot of clinal divergence in species that differed in their arrival times into new ranges to indirectly infer temporal dynamics of cline evolution. However, a true time-series analysis of evolutionary parallelism between native and introduced clines would also be valuable, though such data are sparse. In a rare exception, Wu and Colautti (22) analysed herbarium records to compare clinal patterns of flowering phenology in three introduced ranges of *Lythrum salicaria* over 150 years, and found lags in the evolution of adaptive clines in all three regions. Because herbarium specimens are collected in the field, the contribution of phenotypic plasticity to the trait variation must be controlled (22), although genomic analyses (30) or quantitative genetic approaches can be leveraged to overcome those issues (81). In our meta-analysis, we found that multivariate parallelism was weaker in field studies compared to common garden experiments (though no such differences were observed in the univariate analysis), which suggests that herbarium-based phenotypic cline estimates could be valuable for inferring lower bounds for the evolution of parallelism between ranges.

References

1. J. Arendt, D. Reznick, Convergence and parallelism reconsidered: what have we learned about the genetics of adaptation? *Trends Ecol Evol* **23**, 26–32 (2008).

2. D. L. Stern, The genetic causes of convergent evolution. *Nat Rev Genet* **14**, 751–764 (2013).

3. S. J. Gould, *Wonderful life: the Burgess Shale and the nature of history* (WW Norton & Company, 1989).

4. P. W. Messer, S. P. Ellner, N. G. Hairston, Can population genetics adapt to rapid evolution? *Trends Genet* **32**, 408–418 (2016).

5. A. A. Agrawal, A. P. Hastings, M. T. J. Johnson, J. L. Maron, J.-P. Salminen, Insect herbivores drive real-time ecological and evolutionary change in plant populations. *Science* **338**, 113–116 (2012).

6. R. Gomulkiewicz, D. Houle, Demographic and genetic constraints on evolution. *Am Nat* **174**, E218–E229 (2009).

7. J. Maynard Smith, What determines the rate of evolution? *Am Nat* **110**, 331–338 (1976).

8. J. Polechová, Evolution of species' range and niche in changing environments. *bioRxiv* 2025–01 (2025). https://doi.org/10.1011/2025.01.16.633367.

9. J. Polechová, Is the sky the limit? On the expansion threshold of a species' range. *PLoS Biol* **16**, e2005372 (2018).

10. M. Kirkpatrick, N. H. Barton, Evolution of a species' range. *Am Nat* **150**, 1–23 (1997).

11. C. M. Caruso, *et al.*, What are the environmental determinants of phenotypic selection? A meta-analysis of experimental studies. *Am Nat* **190**, 363–376 (2017).

12. A. M. Siepielski, *et al.*, Precipitation drives global variation in natural selection. *Science* **355**, 959–962 (2017).

13. P. J. Prentis, J. R. Wilson, E. E. Dormontt, D. M. Richardson, A. J. Lowe, Adaptive evolution in invasive species. *Trends Plant Sci* **13**, 288–294 (2008).

14. K. A. Hodgins, P. Battlay, D. G. Bock, The genomic secrets of invasive plants. *New Phytol* **245**, 1846–1863 (2025).

15. L. A. van Boheemen, D. Z. Atwater, K. A. Hodgins, Rapid and repeated local adaptation to climate in an invasive plant. *New Phytol* **222**, 614–627 (2019).

16. J. L. Maron, M. Vilà, R. Bommarco, S. Elmendorf, P. Beardsley, Rapid evolution of an invasive plant. *Ecol Monogr* **74**, 261–280 (2004).

17. J. R. Etterson, *et al.*, Parallel patterns of clinal variation in *Solidago altissima* in its native range in central USA and its invasive range in Japan. *Botany* **86**, 91–97 (2008).

18. W. Liu, X. Chen, J. Wang, Y. Zhang, Does the effect of flowering time on biomass allocation across latitudes differ between invasive and native salt marsh grass *Spartina alterniflora*? *Ecol Evol* **12**, e8681 (2022).

19. W.-W. Liu, Y.-H. Zhang, Geographical variation in germination traits of the salt-marsh cordgrass *Spartina alterniflora* in its invasive and native ranges. *J Plant Ecol* **14**, 348–360 (2021).

20. F. Colomer-Ventura, *et al.*, Contemporary evolution of an invasive plant is associated with climate but not with herbivory. *Funct Ecol* **29**, 1475–1485 (2015).

21. J. M. Alexander, P. J. Edwards, M. Poll, C. G. Parks, H. Dietz, Establishment of parallel altitudinal clines in traits of native and introduced forbs. *Ecology* **90**, 612–622 (2009).

22. Y. Wu, R. I. Colautti, Evidence for continent-wide convergent evolution and stasis throughout 150 y of a biological invasion. *Proc Natl Acad Sci U S A* **119**, e2107584119 (2022).

23. S. G. Innes, J. S. Santangelo, N. J. Kooyers, K. M. Olsen, M. T. J. Johnson, Evolution in response to climate in the native and introduced ranges of a globally distributed plant. *Evolution* **76**, 1495–1511 (2022).

24. R. I. Colautti, J. A. Lau, Contemporary evolution during invasion: evidence for differentiation, natural selection, and local adaptation. *Mol Ecol* **24**, 1999–2017 (2015).

25. O. Bossdorf, *et al.*, Phenotypic and genetic differentiation between native and introduced plant populations. *Oecologia* **144**, 1–11 (2005).

26. E. C. Woods, S. E. Sultan, Post-introduction evolution of a rapid life-history strategy in a newly invasive plant. *Ecology* **103**, e3803 (2022).

27. Y. Yang, *et al.*, Rapid evolution of latitudinal clines in growth and defence of an invasive weed. *New Phytol* **230**, 845–856 (2021).

28. S. G. Innes, J. S. Santangelo, N. J. Kooyers, K. M. Olsen, M. T. J. Johnson, Evolution in response to climate in the native and introduced ranges of a globally distributed plant. *Evolution* **76**, 1495–1511 (2022).

29. P. A. H. Westley, What invasive species reveal about the rate and form of contemporary phenotypic change in nature. *Am Nat* **177**, 496–509 (2011).

30. P. Battlay, *et al.*, Large haploblocks underlie rapid adaptation in the invasive weed *Ambrosia artemisiifolia*. *Nat Commun* **14**, 1717 (2023).

31. G. García-Ramos, M. Kirkpatrick, Genetic models of adaptation and gene flow in peripheral populations. *Evolution* **51**, 21–28 (1997).

32. A. Duputié, F. Massol, I. Chuine, M. Kirkpatrick, O. Ronce, How do genetic correlations affect species range shifts in a changing environment? *Ecol Lett* **15**, 251–259 (2012).

33. T. F. Hansen, D. Houle, Measuring and comparing evolvability and constraint in multivariate characters. *J Evol Biol* **21**, 1201–1219 (2008).

34. Y. E. Stuart, *et al.*, Contrasting effects of environment and genetics generate a continuum of parallel evolution. *Nat Ecol Evol* **1**, 158 (2017).

35. T. A. Mousseau, D. A. Roff, Natural selection and the heritability of fitness components. *Heredity* **59**, 181–197 (1987).

36. M. J. Page, *et al.*, The PRISMA 2020 statement: an updated guideline for reporting systematic reviews. *BMJ* **372**, n71 (2021).

37. C. A. Schneider, W. S. Rasband, K. W. Eliceiri, NIH Image to ImageJ: 25 years of image analysis. *Nat Methods* **9**, 671–675 (2012).

38. F. Essl, *et al.*, A conceptual framework for range-expanding species that track human-induced environmental change. *BioScience* **69**, 908–919 (2019).

39. J. M. Alexander, P. J. Edwards, M. Poll, C. G. Parks, H. Dietz, Establishment of parallel altitudinal clines in traits of native and introduced forbs. *Ecology* **90**, 612–622 (2009).

40. D. Z. Atwater, C. Ervine, J. N. Barney, Climatic niche shifts are common in introduced plants. *Nat Ecol Evol* **2**, 34–43 (2018).

41. H. Seebens, *et al.*, No saturation in the accumulation of alien species worldwide. *Nat Commun* **8**, 14435 (2017).

42. A. Compagnoni, *et al.*, Herbaceous perennial plants with short generation time have stronger responses to climate anomalies than those with longer generation time. *Nat Commun* **12**, 1824 (2021).

43. M. Pacifici, *et al.*, Generation length for mammals. *Nat Conserv* **5**, 89–94 (2013).

44. J. Kattge, *et al.*, TRY plant trait database – enhanced coverage and open access. *Glob Chang Biol* **26**, 119–188 (2020).

45. J. Staerk, *et al.*, Performance of generation time approximations for extinction risk assessments. *J Appl Ecol* **56**, 1436–1446 (2019).

46. R Core Team, R: A Language and Environment for Statistical Computing. R Foundation for Statistical Computing, Vienna, Austria. (2024). Deposited 2024.

47. D. Z. Atwater, C. Ervine, J. N. Barney, Climatic niche shifts are common in introduced plants. *Nat Ecol Evol* **2**, 34–43 (2018).

48. C. Carvalho, *et al.*, Multivariate selection mediated by aridity predicts divergence of drought-resistant traits along natural aridity gradients of an invasive weed. *New Phytol* **234**, 1088–1100 (2022).

49. J. O. Friedrich, N. K. Adhikari, J. Beyene, The ratio of means method as an alternative to mean differences for analyzing continuous outcome variables in meta-analysis: a simulation study. *BMC Med Res Methodol* **8**, 32 (2008).

50. W. Viechtbauer, Conducting meta-analyses in R with the metafor package. *J Stat Softw* **36**, 1–48 (2010).

51. A. F. Zuur, E. N. Ieno, N. J. Walker, A. A. Saveliev, G. M. Smith, "Mixed Effects Modelling for Nested Data" in *Mixed Effects Models and Extensions in Ecology with R*, A. F. Zuur, E. N. Ieno, N. Walker, A. A. Saveliev, G. M. Smith, Eds. (Springer, 2009), pp. 101–142.

52. G. Knapp, J. Hartung, Improved tests for a random effects meta-regression with a single covariate. *Stat Med* **22**, 2693–2710 (2003).

53. M. Harrer, P. Cuijpers, T. Furukawa, D. D. Ebert, dmetar: companion R package for the guide "Doing meta-analysis in R." *R package version 0.0* **9000**, 2019 (2019).

54. V. Calcagno, C. de Mazancourt, glmulti: an R package for easy automated model selection with (generalized) linear models. *J Stat Softw* **34**, 1–29 (2010).

55. K. P. Burnham, D. R. Anderson, Multimodel inference: understanding AIC and BIC in model selection. *Sociol Methods Res* **33**, 261–304 (2004).

56. S. Nakagawa, *et al.*, orchaRd 2.0: An R package for visualising meta-analyses with orchard plots. *Methods Ecol Evol* **14**, 2003–2010 (2023).

57. J. A. Crooks, Lag times and exotic species: The ecology and management of biological invasions in slow-motion1. *Ecoscience* **12**, 316–329 (2005).

58. J. Polechová, N. H. Barton, Limits to adaptation along environmental gradients. *Proc Natl Acad Sci U S A* **112**, 6401–6406 (2015).

59. K. Štajerová, P. Šmilauer, J. Brůna, P. Pyšek, Distribution of invasive plants in urban environment is strongly spatially structured. *Landsc Ecol* **32**, 681–692 (2017).

60. P. M. Groffman, *et al.*, Ecological homogenization of urban USA. *Front Ecol Environ* **12**, 74–81 (2014).

61. L. C. Rigby, M. D. Hall, K. Monro, A. Uesugi, Evolution of "invasion syndrome" in invasive goldenrod is not constrained by genetic trade-offs. *Evol Appl* **17**, e13734 (2024).

62. B. Calsbeek, S. Lavergne, M. Patel, J. Molofsky, Comparing the genetic architecture and potential response to selection of invasive and native populations of reed canary grass. *Evol Appl* **4**, 726–735 (2011).

63. S. J. Franks, G. S. Wheeler, C. Goodnight, Genetic variation and evolution of secondary compounds in native and introduced populations of the invasive plant *Melaleuca quinquenervia*. *Evolution* **66**, 1398–1412 (2012).

64. B. V. McGoey, J. R. Stinchcombe, Introduced populations of ragweed show as much evolutionary potential as native populations. *Evol Appl* **14**, 1436–1449 (2021).

65. Y. Sakata, *et al.*, Environmentally triggered variability in the genetic variance–covariance of herbivory resistance of an exotic plant *Solidago altissima*. *Ecol Evol* **10**, 3103–3111 (2020).

66. B. Zhang, A. Hastings, E. D. Grosholz, L. Zhai, The comparison of dispersal rate between invasive and native species varied by plant life form and functional traits. *Mov Ecol* **11**, 73 (2023).

67. B. L. Phillips, G. P. Brown, R. Shine, Evolutionarily accelerated invasions: the rate of dispersal evolves upwards during the range advance of cane toads. *J Evol Biol* **23**, 2595–2601 (2010).

68. Q. Guo, Central-marginal population dynamics in species invasions. *Front Ecol Evol* **2**, 23 (2014).

69. R. E. Irwin, P. S. Warren, L. S. Adler, Phenotypic selection on floral traits in an urban landscape. *Proc R Soc B Biol Sci* **285**, 20181239 (2018).

70. Ø. Totland, Environment-dependent pollen limitation and selection on floral traits in an alpine species. *Ecology* **82**, 2233–2244 (2001).

71. M. A. Geber, L. R. Griffen, Inheritance and natural selection on functional traits. *Int J Plant Sci* **164**, S21–S42 (2003).

72. M. T. Johnson, A. A. Agrawal, J. L. Maron, J.-P. Salminen, Heritability, covariation and natural selection on 24 traits of common evening primrose (*Oenothera biennis*) from a field experiment. *J Evol Biol* **22**, 1295–1307 (2009).

73. K. A. Hodgins, D. G. Bock, L. H. Rieseberg, Trait evolution in invasive species. *Annual Plant Reviews Online* **1**, 459–496 (2018).

74. B. Blossey, R. Notzold, Evolution of increased competitive ability in invasive nonindigenous plants: a hypothesis. *J Ecol* **83**, 887–889 (1995).

75. A. R. Zangerl, M. C. Stanley, M. R. Berenbaum, Selection for chemical trait remixing in an invasive weed after reassociation with a coevolved specialist. *Proc Natl Acad Sci U S A* **105**, 4547–4552 (2008).

76. Y. Sakata, M. Yamasaki, Y. Isagi, T. Ohgushi, An exotic herbivorous insect drives the evolution of resistance in the exotic perennial herb *Solidago altissima*. *Ecology* **95**, 2569–2578 (2014).

77. R. I. Colautti, S. C. H. Barrett, Rapid adaptation to climate facilitates range expansion of an invasive plant. *Science* **342**, 364–366 (2013).

78. J. G. Oakeshott, *et al.*, Alcohol dehydrogenase and glycerol-3-phosphate dehydrogenase clines in *Drosophila melanogaster* on different continents. *Evolution* **36**, 86–96 (1982).

79. J. R. Adrion, M. W. Hahn, B. S. Cooper, Revisiting classic clines in *Drosophila melanogaster* in the age of genomics. *Trends Genet* **31**, 434–444 (2015).

80. A. A. Hoffmann, A. R. Weeks, Climatic selection on genes and traits after a 100 year-old invasion: a critical look at the temperate-tropical clines in *Drosophila melanogaster* from eastern Australia. *Genetica* **129**, 133–147 (2007).

81. A. S. Kim, *et al.*, Temporal collections to study invasion biology. *Mol Ecol* **32**, 6729–6742 (2023).